ChemComm

COMMUNICATION

View Article Online
View Journal | View Issue

Cite this: *Chem. Commun.*, 2023, **59**, 8830

Received 11th April 2023,
Accepted 12th June 2023

DOI: 10.1039/d3cc01726e

rsc.li/chemcomm

A photoresponsive gold catalyst based on azobenzene-functionalized NHC ligands†

Jianghua Liu, Eduard O. Bobylev, Bas de Bruin and Joost N. H. Reek *

An azobenzene-bearing N-heterocyclic carbene-based gold catalyst is reported of which the reactivity in a cyclization reaction depends on the isomeric state of the azobenzene. The configurations of the catalyst can be reversibly switched by light and are stable during the reaction, effectively leading to a switchable catalyst system.

Development of artificial switchable catalysts allowing control over the rate and selectivity of reactions by external stimuli has emerged as an important research area.[1] The interest has been fueled by the potential in regulating organic transformations in new ways. In addition, stimuli-responsive catalysis in living systems may find application in smart medicine,[2] and as such, transition metal catalysis in living systems has become an emerging frontier in recent years.[3] Switchable catalysts can provide spatial and temporal control in catalysis which may be relevant for diverse applications in synthetic chemistry as well as in biology. Various external stimuli can be used, including light,[4] heat,[5] ultrasound,[6] and even magnetic fields.[7] Among the external stimuli, light[8] is attractive because it is a clean, non-invasive stimulus, and it can remotely control reactions in time and space. Photoswitchable organometallic catalysts containing photochromic ligands (*i.e.* spiropyran, azobenzene, diarylethenes, biindanes, *etc.*) and transition metal centers (*i.e.* Rh, Ru, Au, Cu, Pd and *etc.*) have been reported, and applied in organic solvents.[9]

Azobenzene (Azo) is the most widely studied photoresponsive group.[10] It can be reversibly switched between *trans* and *cis* configurations under UV light and visible light, and also heating can be used for isomerization from *cis* to *trans*. As photoisomerization changes the configurations of azobenzene, it may provide useful handle for regulating reactions by light-controlled steric effects.[11] Gold complexes are increasingly popular as catalyst as they display unique reactivity[12] and allow a variety of cyclization reactions under mild conditions.[13] In addition, gold complexes typically display low toxicity[14] and have reactivity that is complementary to reactions found in nature,[15] and therefore they have been used under biorelevant conditions.[16] We have reported previously switchable gold catalysts by encapsulation of the complex, which effectively shifted the equilibrium from dinuclear to mononuclear.[17] However, photoswitchable gold complexes used as catalysts for cyclization reactions under mild conditions have not been reported so far.

Here, we report an N-heterocyclic carbene (NHC) ligand[18] with two azobenzene functional groups as photoswitchable units, and the coordination to gold to form a complex (Azo-NHC-Au) that can be used in catalysis. The azobenzene units can be switched with light and this in turn controls the activity of the gold complex in a cyclization reaction. The *trans* and *cis* configurations of the Azo-NHC-Au catalysts can be interconverted by irradiation with UV and visible light (Scheme 1). The *trans* Azo-NHC-Au complex displays rates that are more than two times higher compared to that of the *cis*-isomer.

The photoswitchable bis-azobenzene N-heterocyclic carbene ligand and the gold complex (Azo-NHC-Au) thereof were synthesized[19] using standard procedures and fully characterized by ^{1}H NMR, ^{13}C NMR and FD-Mass (See Supplementary, Scheme S1 and Fig. S1–S6, ESI†). The ligand (Azo-NHC) and gold complex (Azo-NHC-Au) are isolated as the thermodynamically stable *trans*-L isomer and *trans*-Cat, respectively, as confirmed by the absorption band at 320 nm in UV-vis (Fig. 1b). The photoisomerization

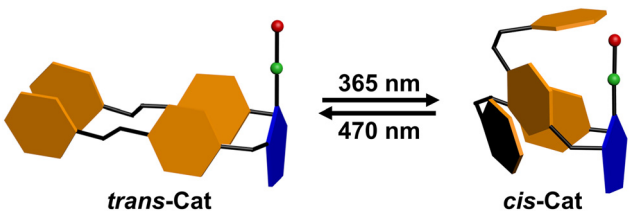

Scheme 1 Light controlled isomerization of the Azo-NHC-Au complex.

Homogeneous, Supramolecular and Bio-Inspired Catalysis (HomKat), Van 't Hoff Institute for Molecular Sciences (HIMS), University of Amsterdam (UvA), Science Park 904, Amsterdam 1098XH, The Netherlands. E-mail: j.n.h.reek@uva.nl

† Electronic supplementary information (ESI) available. See DOI: https://doi.org/10.1039/d3cc01726e

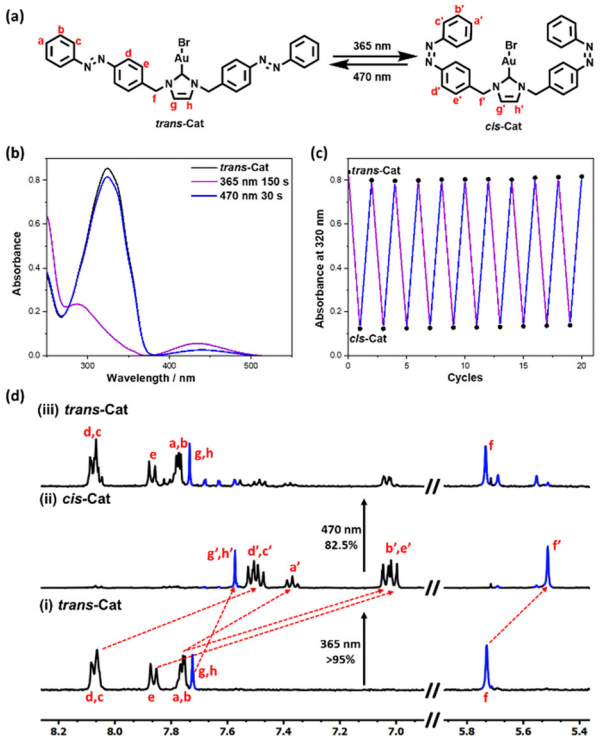

Fig. 1 (a) Photoswitching between *trans*-Cat and *cis*-Cat; (b) UV-vis absorption spectrum of *trans*-Cat and the photoswitched state to give *cis*-Cat in THF:H_2O; (c) Multiple switching between *trans*-Cat and *cis*-Cat monitored by UV-vis absorption at 320 nm; (d) Part of the ^{1}H NMR spectra (400 MHz, THF-d_8:D_2O = 1 : 1, 298 K) of (i) *trans*-Cat, (ii) *cis*-Cat, obtained from (i) by irradiating by 365 nm light for 300 s, (iii) *trans*-Cat, obtained from (ii) irradiating by 470 nm light for 30 s (UV-vis: [*trans*-Cat] = 20 μM in THF:H_2O = 1 : 1 at 298 K; ^{1}H NMR: [*trans*-Cat] = 500 μM in THF-d_8:D_2O = 1 : 1 at 298 K).

of the catalyst was investigated by ^{1}H NMR and UV-vis spectroscopy. *Trans*-Cat has a maximum absorption at 320 nm, characteristic of the *trans* azobenzene unit (Fig. 1b and Fig. S9, ESI†). Upon irradiation of a THF:H_2O = 1 : 1 solution of the *trans*-Cat with 365 nm light, this 320 nm absorption band decreased, while a new band at 440 nm, typical for the *cis*-azobenzene (*cis*-Azo), arises (Fig. S9b, ESI†), indicating that *trans* to *cis*- isomerization efficiently occurred. The photostationary state (PSS) is achieved after 150 s 365 nm irradiation and contains 95% *cis*-Azo and 5% *trans*-Azo as calculated by Abs(PSS)/Abs(*trans*-Azo) ratio (Fig. S10, ESI†).[20] Exposing the solution after this period of time to 470 nm light leads to a decrease of the 440 nm band (associated to *cis*-Azo) and an increase of the 320 nm absorbtion (the band of the *trans*-Azo) again. This experiment shows that the *trans*-Cat can be reformed and the PSS state was now reached after irradiation for 30 s at 470 nm (Fig. S9c, ESI†). Importantly, the reversible isomerization of the catalyst could be repeated at least ten times without any signs of degradation (Fig. 1c and Fig. S9d, ESI†). Similar photoisomerization experiments on the Azo-NHC ligand showed that it has similar photochromic behavior as observed for the catalyst (Fig. S7 and S8, ESI†).

Next, the isomerization conversion efficiency of the Azo-NHC-Au complex was quantitatively studied by ^{1}H NMR (Fig. 1d). Under ^{1}H NMR conditions, the PSS state was reached after 300 s exposure to 365 nm light. The peaks of *trans*-Cat almost completely disappeared while a new set of signals attributed to the *cis*-Cat appeared. Based on the integrals of the peaks attributed to f (or g, h) with respect to f′ (or g′, h′), the conversion efficiency from *trans*-Azo to *cis*-Azo was calculated to be more than 95%. After irradiating the solution by blue light for 30 s, the conversion *of cis*-Azo to *trans*-Azo was determined as 82.5%. The isomerization efficiency calculated by ^{1}H NMR is similar to those based on the UV-vis experiments.

Next, we monitored the isomerization process in time by ^{1}H NMR spectroscopy, to see if the photoisomerization of *trans*-Cat to *cis*-Cat proceeds *via* an isomer in which only one of the azobenzene units is switched (*trans-cis*-Cat) (Fig. 2). After irradiation of the solution containing the *trans*-Cat isomer for 60 s with 365 nm light, the signals attributed to both the *trans*-Cat and the *cis*-Cat are clearly visible (*i.e.*, protons on imidazolium ring (H_g and H_h) and CH_2 (H_f)) for *trans*-Cat and ($H_{g'}$, $H_{h'}$ and $H_{f'}$) for *cis*-Cat). Next to this a new set of signals is clearly visible ($H_{g''}$, $H_{h''}$, $H_{f_1''}$ and $H_{f_2''}$, in green in Fig. 2), which is attributed to the intermediate *trans-cis*-Cat. The first PSS is reached after irradiation with 365 nm for 300 s, and NMR shows that the ratio of these three configurations is 0 : 9 : 91 based on the integrals of f, f_1'', f_2'' f′ (*trans*-Cat:*trans-cis*-Cat:*cis*-Cat). Irradiation of this solution containing dominantly *cis*-Cat with 470 nm light for 5 s, shows that also this pathway proceeds *via* the *trans-cis*-Cat intermediate. After irradiation with 470 nm light for 30 s, another PSS state was obtained with the isomers present in the ratio 65 : 31 : 4 (*trans*-Cat:*trans-cis*-Cat:*cis*-Cat).

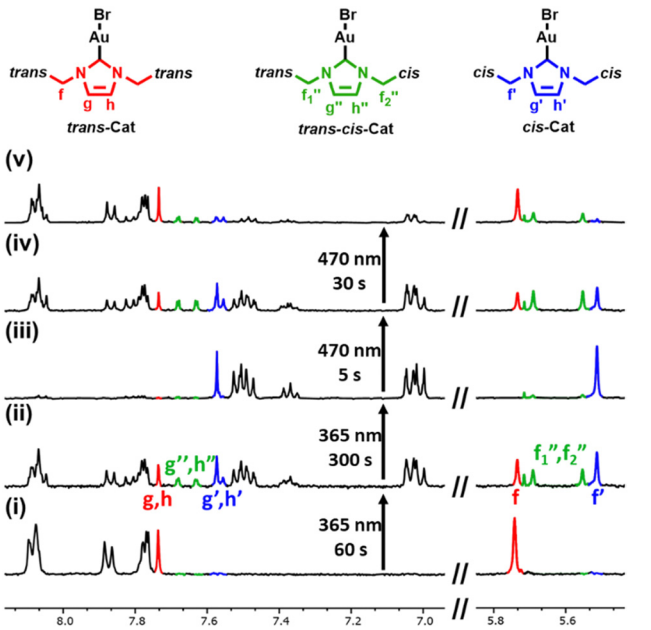

Fig. 2 Part of ^{1}H NMR spectra (400 MHz, THF-d_8:D_2O = 1 : 1, 298 K) of catalyst (i) *trans*-Cat, (ii) mixture obtained from (i) irradiating by 365 nm light for 60 s, (iii) mixture solution obtained from (i) irradiating by 365 nm light for 300 s, (iv) mixture solution obtained from (iii) irradiating by 470 nm light for 5 s, (v) mixture solution obtained from (iii) irradiating by 470 nm light for 30 s. ([*trans*-Cat] = 500 μM in THF-d_8:D_2O = 1 : 1 at 298 K).

Next, the thermal relaxation of *cis*-Cat was studied by monitoring the solution, which is kept in the dark, every 1 h for 24 h by UV-vis and ^{1}H NMR (Fig. S11, ESI†). Surprisingly, only 5% *cis*-Cat was thermally relaxed to *trans*-Cat after 24 h at dark, which is unusually slow compared to normal azobenzene. The typical thermal half-life of the *Z*-isomers of azobenzene at room temperature in acetonitrile is 4.7 h.[21] Previously it has established that thermal stability of the *Z*-isomers can be improved by electronic effects, for example, the ortho fluoro-azobenzenes are configurational more stable than the parent azobenzene.[22] DFT calculations, show π–π stacking of benzene rings between two azobenzene units in the *cis*-Cat structure (Fig. 4), which might explain the thermostability of the ligands in the *cis* state (*vide infra*). This high thermal stability is crucial for the application in catalysis as it allows to use the *cis*-Cat sufficiently long for allowing significant substrate conversion.

To evaluate the catalytic performance of the *trans*-Cat and *cis*-Cat, the intramolecular cyclization of acetylenic acid was explored (Fig. 3a). We used conditions that do not require silver(I) salts to remove the halide from the gold catalyst,[13,16,23] as silver is sensitive to the light that we use for photoisomerization. To that end water was used as co-solvent as it is known to activate gold complexes by bromide replacement. As such, the catalytic reactions were performed in THF-d_8:D_2O = 1 : 1 at room temperature and conversions were monitored every hour by ^{1}H NMR for 24 h. The yield and rate constant k of the catalytic reactions as function of time are displayed in Fig. 3a and b and Fig. S12–S14 (ESI†). The *trans*-Cat shows good catalytic activity (k = 0.081 h^{-1}) and provided 87% yield after 16 h. Under the same conditions using the *cis*-Cat, which was obtained by 365 nm light irradiating of the *trans*-Cat solution for 10 min, the reaction rate was much slower (k = 0.035 h^{-1}) with 52% yield after 16 h, showing that the catalyst activity can be switched by light. The concentration of *trans*-Cat and *cis*-Cat during the reactions were also monitored based on the integrals of proton f. The unchanged concentrations during these experiments demonstrate the excellent geometric stability of both *trans*-Cat and *cis*-Cat under the reaction conditions.

The different reactivity displayed by *trans*-Cat and *cis*-Cat may be caused by the difference in steric hindrance of the ligand. Density functional theory (DFT) calculations (BP86, def2-SVP, D3 dispersion corrections, see ESI† for details) were carried out to investigate the effect of the configurations of the ligand. The input structures of the *trans*-Cat and *cis*-Cat complexes were pre-optimized with GFN2-*x*TB, and subsequently a conformational search was performed using the crest procedure, and the DFT-optimized the structures of *trans*-Cat and *cis*-Cat are displayed in Fig. 4. The Balls and stick model of *trans*-Cat clearly shows that the two azobenzene arms are parallel oriented to allow face-to-face stacking of the aromatic rings. The azobenzene in *cis*-Cat structure are arranged such that they form a face to edge stacking arrangement (Fig. 4a and b). The different orientation of the rings in the *trans*-Cat and *cis*-Cat creates a different steric environment around the gold center in the area where the substrate should coordinate. Clearly, the space-filling model, topographic steric map and %buried volume (%V_{Bur}) (Fig. S21, ESI†) of *trans*-Cat visualizes the larger

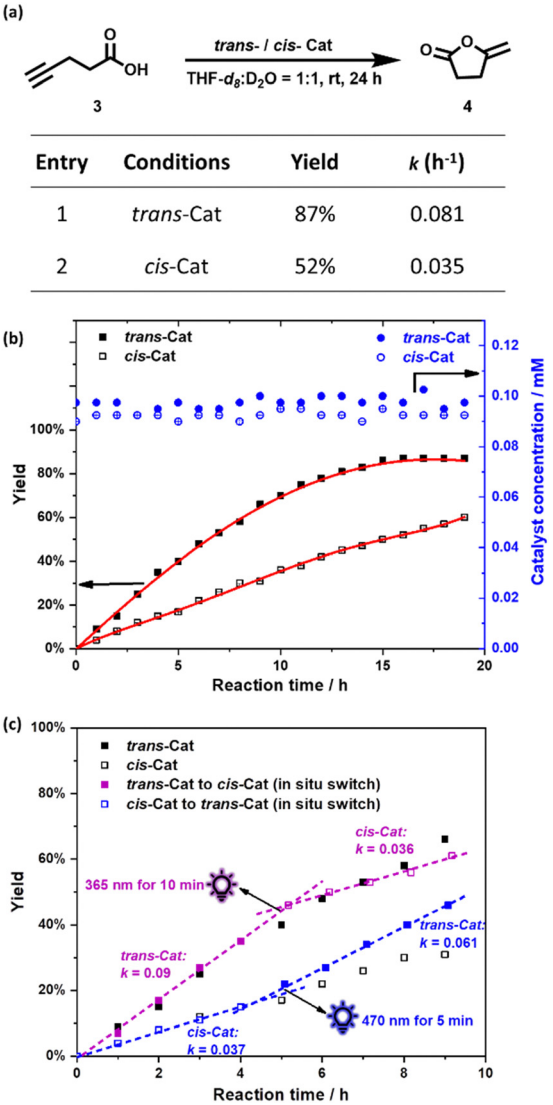

Entry	Conditions	Yield	k (h^{-1})
1	*trans*-Cat	87%	0.081
2	*cis*-Cat	52%	0.035

Fig. 3 (a) Cyclization reaction of acetylenic acid **3** to give enol lactone **4**, with the yield and rate constant k displayed in the table; (b) The yield as function of time determined by ^{1}H NMR spectroscopy in red and the concentration of the catalyst during the reaction (THF-d_8:D_2O = 1 : 1 at 298 K); (c) *In situ* photoswitchable catalysis: (purple) switch from *trans*-Cat to *cis*-Cat, after 4 h (by 10 min irradiation 365 nm). (blue) switch from *cis*-Cat to *trans*-Cat, after 4 h (by 5 min irradiation with 470 nm). Conditions: Reagent concentrations: [**3**] = 1 mM, [*trans*- or *cis*-Cat] = 0.1 mM. The yield was determined by ^{1}H NMR using 1,3,5-trimethoxybenzene as an internal standard (error <5%). For full experimental details see the ESI.†)

available area for coordination in the *trans*-Cat compared to *cis*-Cat, which may explain the difference in reaction rate for the cyclization (Fig. 4c and d).

Finally, we explored if the reaction activity could be regulated by photoswitching the catalysts *in situ*. Firstly, the reaction started in the presence of the *trans*-Cat for 4 h, showing a similar yield (35%) and rate constant (k = 0.09) previously obtained for *trans*-Cat (k = 0.081). Then the reaction mixture was irradiated by 365 nm light for 10 min to obtain *cis*-Cat to slow down the reaction rate (k = 0.036) (Fig. 3c purple and Fig. S15 and S16, ESI†). In the next experiment, the reaction

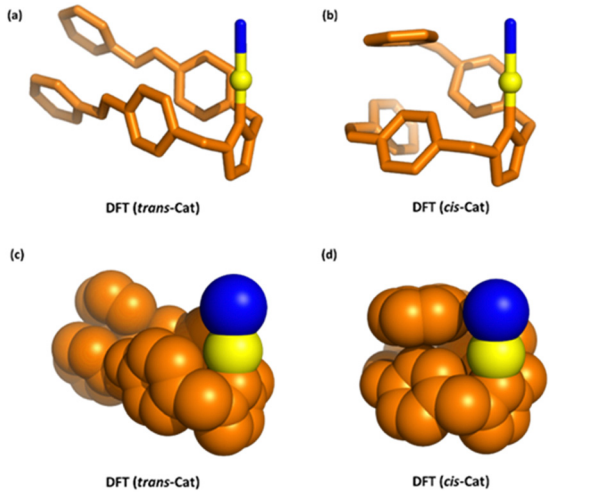

Fig. 4 DFT-optimized structures of (a) *trans*-Cat and (b) *cis*-Cat (ball and sticks models); (c) *trans*-Cat and (d) *cis*-Cat (space filling models). The hydrogens atoms have been omitted for clarity. Orange represents azobenzene and imidazolium ring; Yellow represents gold; Blue represents Br.

started with the *cis*-Cat for 4 h (k = 0.037). Then *trans*-Cat was obtained by 470 nm irradiating 5 min to accelerate the reaction rate to k = 0.061 (Fig. 3c blue and Fig. S17 and S18, ESI†). No products was found if the substrate solution without catalyst was irradiated with UV or blue light (Fig. S19 and S20, ESI†). These results show that reaction rate can be reversibly controlled by different light conditions.

In conclusion, we report an azobenzene-bearing N-heterocyclic carbene that can be reversibly switched from the *trans* to the *cis* configurations using light, also when coordinated to gold. The *trans*-Cat exhibited almost two times the catalytic activity compared to the *cis*-Cat. The configurations of catalysts can be reversibly switched between *trans*- and *cis*- under reaction conditions, and maintain stable during the reaction process. As gold-catalyzed cyclization reactions are of great significance for various applications including smart drugs and other biological processes, we think this photoswitchable catalyst may have potential to control catalytic reactions spatially and temporally in biological systems. As N-heterocyclic carbene ligands are used for many different catalytic processes we foresee that this ligand may be more broadly applicable.

We gratefully acknowledge the University of Amsterdam and China Scholarship Council (CSC; No. 201906200131) for financial support.

Conflicts of interest

There are no conflicts to declare.

Notes and references

1 (*a*) V. Blanco, D. A. Leigh and V. Marcos, *Chem. Soc. Rev.*, 2015, **44**, 5341–5370; (*b*) M. Vlatković, B. S. L. Collins and B. L. Feringa, *Chem. – Eur. J.*, 2016, **22**, 17080–17111; (*c*) J. Choudhury, *Tetrahedron Lett.*, 2018, **59**, 487–495; (*d*) U. Lüning, *Angew. Chem., Int. Ed.*, 2012, **51**, 8163–8165; (*e*) Y. Tang, Y. He and Q. Fan, *Chin. J. Org. Chem.*, 2020, **40**, 3672–3685.
2 D. Jiang, D. Ni, Z. T. Rosenkrans, P. Huang, X. Yan and W. Cai, *Chem. Soc. Rev.*, 2019, **48**, 3683–3704.
3 (*a*) P. K. Sasmal, C. N. Streu and E. Meggers, *Chem. Commun.*, 2013, **49**, 1581–1587; (*b*) Y. Bai, J. Chen and S. C. Zimmerman, *Chem. Soc. Rev.*, 2018, **47**, 1811–1821; (*c*) M. Martínez-Calvo and J. L. Mascareñas, *Coord. Chem. Rev.*, 2018, **359**, 57–79; (*d*) M. O. N. van de L'Isle, M. C. Ortega-Liebana and A. Unciti-Broceta, *Curr. Opin. Chem. Biol.*, 2021, **61**, 32–42; (*e*) A. H. Ngo, S. Bose and L. H. Do, *Chem. – Eur. J.*, 2018, **24**, 10584–10594; (*f*) D. P. Nguyen, H. T. H. Nguyen and L. H. Do, *ACS Catal.*, 2021, **11**, 5148–5165; (*g*) Y. Liu and Y. Bai, *ACS Appl. Bio Mater.*, 2020, **3**, 4717–4746.
4 S. Neri, S. G. Martin, C. Pezzato and L. J. Prins, *J. Am. Chem. Soc.*, 2017, **139**, 1794–1997.
5 (*a*) H. Ye, K. Yang, J. Tao, Y. Liu, Q. Zhang, S. Habibi, Z. Nie and X. Xia, *ACS Nano*, 2017, **11**, 2052–2059; (*b*) D. E. Bergbreiter, V. M. Mariagnanam and L. Zhang, *Adv. Mater.*, 1995, **7**, 69.
6 W. P. Li, C. H. Su, Y. C. Chang, Y. J. Lin and C. S. Yeh, *ACS Nano*, 2016, **10**, 2017–2027.
7 J. Lee, S. Dubbu, N. Kumari, A. Kumar, J. Lim, S. Kim and I. S. Lee, *Nano Lett.*, 2020, **20**, 6981–6988.
8 Y. Tao, H. F. Chan, B. Shi, M. Li and K. W. Leong, *Adv. Funct. Mater.*, 2020, **30**, 2005029.
9 (*a*) Z. Freixa, *Catal. Sci. Technol.*, 2020, **10**, 3122–3139; (*b*) M. Kondo, K. Nakamura, C. G. Krishnan, H. Sasai and S. Takizawa, *Chem. Rec.*, 2023, e202300040; (*c*) P. J. Gilissen, X. Chen, J. D. Graaf, P. Tinnemans, B. L. Feringa, J. A. Elemans and R. J. Nolte, *Chem. – Eur. J.*, 2023, e202203539.
10 F. A. Jerca, V. V. Jerca and R. Hoogenboom, *Nat. Rev. Chem.*, 2022, **6**, 51–69.
11 (*a*) C. Z.-J. Ren, P. Solís Muñana, J. Dupont, S. S. Zhou and J. L.-Y. Chen, *Angew. Chem.*, 2019, **131**, 15398–15402; (*b*) A. Kunfi, I. Jablonkai, T. Gazdag, P. J. Mayer, P. P. Kalapos, K. Németh, T. Holczbauer and G. London, *RSC Adv.*, 2021, **11**, 23419–23429; (*c*) S. Park, S. Byun, H. Ryu, H. Hahm, J. Lee and S. Hong, *ACS Catal.*, 2021, **11**, 13860–13865; (*d*) T. Arif, C. Cazorla, N. Bogliotti, N. Saleh, F. Blanchard, V. Gandon, R. Métivier, J. Xie, A. Voituriez and A. Marinetti, *Catal. Sci. Technol.*, 2018, **8**, 710–715.
12 (*a*) M. Mato, A. Franchino, C. G. Morales and A. M. Echavarren, *Chem. Rev.*, 2021, **121**(14), 8613–8684; (*b*) A. S. K. Hashmi, *Chem. Rev.*, 2007, **107**, 3180–3211; (*c*) B. Huang, M. Hu and F. D. Toste, *Trends Chem.*, 2020, **2**(8), 707–720; (*d*) D. J. Gorin, B. D. Sherry and F. D. Toste, *Chem. Rev.*, 2008, **108**, 3351–3378; (*e*) S. Witzel, A. S. K. Hashmi and J. Xie, *Chem. Rev.*, 2021, **121**, 8868–8925.
13 (*a*) K. Belger and N. Krause, *Eur. J. Org. Chem.*, 2015, 220–225; (*b*) M. J. Rodríguez-Álvarez, C. Vidal, S. Schumacher, J. Borge and J. García-Álvarez, *Chem. – Eur. J.*, 2017, **23**, 3425–3431.
14 Y. Wang, M. Liu, R. Cao, W. Zhang, M. Yin, X. Xiao, Q. Liu and N. Huang, *J. Med. Chem.*, 2013, **56**, 1455–1466.
15 A. S. K. Hashmi and M. Rudolph, *Chem. Soc. Rev.*, 2008, **37**, 1766–1775.
16 (*a*) T. C. Chang, K. Vong, T. Yamamoto and K. Tanaka, *Angew. Chem., Int. Ed.*, 2021, **60**, 12446–12454; (*b*) C. Vidal, M. Tomás-Gamasa, P. Destito, F. López and J. L. Mascareñas, *Nat. Commun.*, 2018, **9**, 1–9.
17 (*a*) A. C. H. Jans, A. Gómez-Suárez, S. P. Nolan and J. N. H. Reek, *Chem. – Eur. J.*, 2016, **22**, 14836–14839; (*b*) A. C. H. Jans, X. Caumes and J. N. H. Reek, *ChemCatChem*, 2019, **11**, 287–297.
18 S. D. Gonzaez, N. Marion and S. P. Nolan, *Chem. Rev.*, 2009, **109**, 3612–3676.
19 F. Nahra, N. V. Tzouras, A. Collado and S. P. Nolan, *Nat. Protoc.*, 2021, **16**, 1476–1493.
20 C. Y. Huang, A. Bonasera, L. Hristov, Y. Garmshausen, B. M. Schmidt, D. Jacquemin and S. Hecht, *J. Am. Chem. Soc.*, 2017, **139**, 15205–15211.
21 X. M. Liu, X. Y. Jin, Z. X. Zhang, J. Wang and F. Q. Bai, *RSC Adv.*, 2018, **8**, 11580–11588.
22 (*a*) D. Bléger, J. Schwarz, A. M. Brouwer and S. Hecht, *J. Am. Chem. Soc.*, 2012, **134**, 20597–20600; (*b*) C. Knie, M. Utecht, F. Zhao, H. Kulla, S. Kovalenko, A. M. Brouwer, P. Saalfrank, S. Hecht and D. Bléger, *Chem. – Eur. J.*, 2014, **20**, 16492–16501.
23 A. Franchino, M. M. Magraner and A. M. Echavarren, *Bull. Chem. Soc. Jpn.*, 2021, **94**, 1099–1117.